Author: Elbaz M.S.M.M.
Title: Three-dimensional in-vivo intra-cardiac vortex flow from 4D Flow MRI : quantification, automatic identification and association with energy loss
Issue Date: 2016-09-06

Chapter 6

Automatic extraction of the 3D left ventricular diastolic transmitral vortex ring from 3D whole-heart phase contrast MRI using Laplace-Beltrami signatures

This chapter was adapted from:

ElBaz, M. S., Lelieveldt, B. P., Westenberg, J. J., & van der Geest, R. J. (2014). **Automatic extraction of the 3D left ventricular diastolic transmitral vortex ring from 3D whole-heart phase contrast MRI using Laplace-Beltrami signatures.** In *Statistical Atlases and Computational Models of the Heart. Imaging and Modelling Challenges STACOM-MICCAI (pp. 204-211). Springer Berlin Heidelberg.*

Abstract

In this work, a new method is proposed for automatic extraction of the left ventricular diastolic transmitral vortex ring from 3D whole-heart three directional Phase Contrast MRI. The proposed method consists of two parts, training and extraction. In the training step, an average reference signature of the complex transmitral vortex ring is captured from training subjects using Laplace-Beltrami spectrum and the Lambda2 method. In the vortex extraction step, the trained signature is used to identify the vortex ring by performing an iterative search for the vortex object with minimum distance from the trained signature. The proposed method is validated on a dataset of 8 healthy volunteers with 32 observed diastolic vortex rings. The method was able to successfully extract 27 diastolic vortex rings from a total of 32. Furthermore, the conducted experiments showed the capability of the proposed method in dealing with vortex shape changes that occur between the phases of early and late diastolic filling.

6.1. Introduction

Vortex formation in intra-cardiac flow patterns has recently gained much interest due to its vital role in keeping balance between blood motion and stresses of sur-rounding structures. Vortices are complex flow structures that evolve as a result of a change in velocity direction around an imaginary axis. In the cardiac Left Ventricle (LV), during early and late diastolic filling, the flow behind the mitral valve develops as a closed vortex tube: a vortex ring [1]. Vortex rings are frequently observed in nature because of their stability [1]. Recent studies have shown that transmitral vortex rings evolve in the LV during rapid early filling (**E**-wave) and late filling (**A**-wave) [2, 3]. These vortex rings help in improving blood transport through the ventricle towards the aorta, minimizing the loss of energy and preventing blood stagnation [1, 2, 4]. Moreover, patients with diastolic dysfunction have been shown to form different diastolic vortex rings compared to healthy volunteers [5-7]. This makes vortex ring analysis a promising tool for detection of diastolic blood flow abnormalities. Nevertheless, most of the reported studies are based on Computational Fluid Dynamics (CFD) simulations [1, 4] or Echocardiography [5, 6]. CFD simulations usually require simplifications of the anatomy (i.e. cardiac chambers) or boundary conditions, which might result in simulated blood flow velocities different from the actual flow. In echocardiography, generally only one single velocity component out of the three velocity components can be acquired providing limited flow velocity information.

Phase Contrast MRI (PC-MRI), also referred to as Velocity-Encoded MRI, can acquire all the three directional velocity components (in-plane and through-plane) of the blood flow relative to the three spatial dimensions and over the cardiac cycle, providing a powerful tool for cardiac flow analysis. In [7], Toger et al. used PC-MRI flow data to measure diastolic vortex ring volume using manual delineation of the vortex ring boundary from visualized Lagrangian coherent structures. They used the measured vortex volumes to differentiate between healthy volunteers and patients with dilated ischemic cardiomyopathy. In [8],Eriksson et al. proposed to quantify the intraventricular cardiac blood flow based on the visualization of PC-MRI data using pathline extraction, which allowed them to subdivide the intracardiac flow into four components based on their rates of passage relative to the cardiac cycle. In [9, 10] flow visualization techniques (e.g. particle tracing, stream lines, streaklines,…etc) for PC-MRI flow were used to qualitatively assess the aorta function. Nevertheless, in most of these studies, vortex rings were defined qualitatively using flow visualization techniques (e.g. as region of swirling pathlines or steamlines), which might suffer from observer bias or high cluttered data. In [11], ElBaz et al. used the lambda2 method which is a quantitative method to define vortex rings. However, vortex rings were then extracted manually which is a tedious and time consuming process.

Due to the complex intra-cardiac blood flow, vortex rings are neither the only nor always the largest vortex object in the heart. Thus, using simple metrics (e.g. vortex size or location) is not enough to extract the LV vortex ring from surrounding vortex structures, similar in size, close in space, but different in shape. Furthermore, cardiac vortex rings are not ideally shaped rings but rather complex structures that tend to have a quasi-ring-like shape (Figure 6.1). All these factors make automatic vortex ring extraction from PC-MRI flow data a difficult and challenging task.

In this paper, we propose a novel method for automatic extraction of diastolic transmitral vortex rings from three-directional, three dimensional time resolved Phase Contrast MRI flow data during the rapid early (**E**) and late (**A**) filling phases. In the proposed work, we use a cardiac-vortex-specific shape signature to tackle the complex cardiac vortex shape and structure problems.

The proposed method consists of two parts. First, vortex structures are identified from the PC-MRI flow field using the Lambda2 method [12]. From this, a cardiac vortex ring signature is defined using the Laplace-Beltrami spectrum method [13]. Second, the cardiac vortex is extracted from the PC-MRI flow field by searching iteratively for the object with the best signature match relative to the reference signature. To the best of our knowledge, this work is the first attempt to extract vortex rings automatically from Phase Contrast MRI flow data in general and from the LV in particular.

6.2. Methodology

6.2.1. Vortex identification using the Lambda2 method

The first step towards vortex ring extraction is to identify vortex structures from the MRI flow field. To achieve this, we use the Lambda2 method [13] to detect vortex cores as it is considered the most accepted vortex identification technique [1]. Furthermore, the Lamda2 method is a quantitative detection method, i.e. it does not depend on visualization techniques but rather on the physical fluid dynamics definition of the vortex structure. The input for the Lambda2 method are the three velocity components of the velocity vector field. Let U, V and W denote the three velocity components of the flow field acquired using PC-MRI and X, Y, Z denote the three spatial dimensions. Then the Lambda2 method can be applied as follows. First, the velocity gradient tensor **J** is computed as

$$\mathbf{J}=\begin{bmatrix} \frac{\partial u}{\partial x} & \frac{\partial u}{\partial y} & \frac{\partial u}{\partial z} \\ \frac{\partial v}{\partial x} & \frac{\partial v}{\partial y} & \frac{\partial v}{\partial z} \\ \frac{\partial w}{\partial x} & \frac{\partial w}{\partial y} & \frac{\partial w}{\partial z} \end{bmatrix} \quad (1)$$

Second, the tensor **J** is decomposed into its symmetric part, the strain deformation tensor $\mathbf{S} = \frac{\mathbf{J}+\mathbf{J}^{\mathrm{T}}}{2}$ and the antisymmetric part, the spin tensor $\boldsymbol{\Omega} = \frac{\mathbf{J}-\mathbf{J}^{\mathrm{T}}}{2}$, where T is the transpose operation. Then, eigenvalue analysis is applied only on $\mathbf{S}^2 + \boldsymbol{\Omega}^2$**.** Finally**,** a voxel is labeled as part of a vortex core only if it has two negative eigenvalues i.e. if $\lambda_1, \lambda_2, \lambda_3$ are the eigenvalues whereas $\lambda_1 \geq \lambda_2 \geq \lambda_3$ then a voxel is labeled as vortex core if its $\lambda_2 < 0$. However, usually the velocity data is noisy, and as a result of which $\lambda_2 < 0$ gives cluttered results. Therefore, a λ_2 threshold, $\mathrm{T}_{\lambda_2} < 0$, is applied instead to allow separation of strong vortex structures from weaker ones. Using the detected vortex voxels, a vortex structure is defined as connected region of these voxels. In this work, we used connected component analysis (CCA) [14] to define the connected vortex cores. The CCA performance is governed by the threshold T_{λ_2} i.e. it is important that T_{λ_2} results in separate vortex structures for CCA to be able to define them as seperate objects. The Lambda2 method yields the vortex structures in the flow field. These vortex structures are usually visualized as isosurfaces with T_{λ_2} as the isovalue.

It is important to note that the Lambda2 method detects all vortex structures from the flow field i.e. vortex rings may be included in the extracted vortices but not all extracted vortices are vortex rings. The output of this step is converted to isosurfaces of the detected vortex structures from the PC-MRI flow field data (Figure 6.1). The vortex shape signature is subsequently captured by applying the Laplace-Beltrami method to these isosurface meshes.

6.2.2. Capturing Vortex Ring Shape Signature using Laplace-Beltrami Spectrum

From Figure 6.1, it is obvious that cardiac vortex rings are rather complex structures which tend to have a quasi-ring-like shape. Therefore, a method for extraction of cardiac vortex rings should capture the features specific for cardiac vortex rings. We achieve this by using the recently introduced Laplace-Beltrami spectral shape signature [13]. This spectral shape signature is a global shape signature computed only from the object's inherent geometry (e.g. curvature, surface area and volume). Furthermore, this signature can be used to compare objects independent of their representation, position and size. This signature is defined as the beginning sequence of the Laplace-Beltrami (LB) differential operator. That is, for a given manifold $\boldsymbol{M}$ **,** if the LB operator is denoted by Δ, then the Laplacian eigenvalue equation can be written as :

$$\Delta f = -\lambda f \tag{2}$$

where λ is a real scalar value corresponding to the eigenvalue of the Laplacian Δ and f corresponds to its eigenvectors. The shape spectral signature is then defined as the diverging sequence of eigenvalues $0 < \lambda_1 \leq \lambda_2 \leq \lambda_3 \leq \cdots + \infty$. This spectrum is truncated at the **d**th eigenvalue where **d** is application specific, and determined empirically. In our case, we apply the LB operator on the Lambda2 vortex isosurfaces which are discrete triangle meshes, hence, we solve (2) using a finite element method and apply the discrete Laplace-Beltrami (LB) operator and follow the same procedure as described in [13] to capture the LB spectrum for the vortex isosurface.

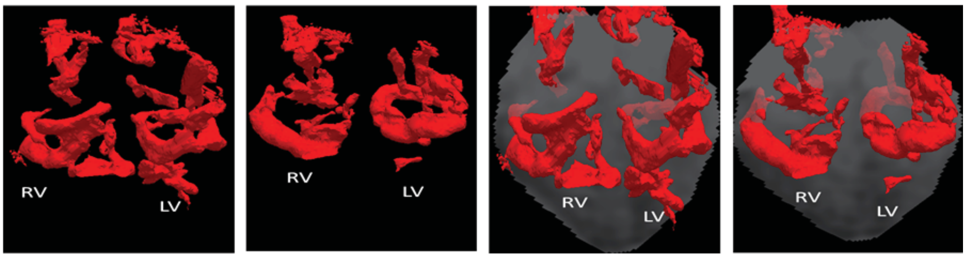

(a) (b) (c) (d)

Figure 6.1. (a, b) Lambda2 isosurfaces of peak early filling (**E**) and late filling (**A**) phases respectively (c,d) their respective heart position in whole heart region of interest magnitude images.

Though similar, cardiac vortex rings differ between subjects. Therefore, we derive an averaged signature from multiple subjects using Laplace-Beltrami analysis as follows. First, for each training subject, the peak early filling (**E** phase) transmitral vortex ring isosurface is manually selected from the identified vortex structures. Second, for each extracted vortex, the Laplace-Beltrami signature is captured as described above. Then, every signature is normalized by both slope of its fitting line and the volume of the vortex isosurface (i.e. the number of voxels in the isosurface) [6]. The reason for this normalization is to make signatures scale invariant. Finally, signature average is computed. Through the rest of the paper we denote the computed vortex shape signature average by **VS.** Due to the representation, position and size invariance properties of the LB signature [13], no shape registration is required prior to averaging. The steps for the vortex ring signature extraction from one subject are illustrated in Figure 6.2.

Of note, in addition to the **E**-phase averaged signature, we tested a signature trained on shapes of both phases (**E** and **A**) vortex rings. However, this provided identical results as for using only **E**-phase averaged signature.

6.2.3. Vortex Ring Extraction

The vortex ring extraction starts by identifying the vortex structures from the PC-MRI data using Lambda2 method as explained in section 6.2.1 Then, the normalized signature of each vortex object in the desired frame is captured using Laplace-Beltrami spectral shape analysis as explained in the previous section. For each vortex object in the current frame, its signature distance $\boldsymbol{D_{sig}}$ from the reference signature **VS** is computed as the L2 norm and computed as:

6

$$\boldsymbol{D_{sig}}(m) = \sum(\mathrm{g_m} - \mathbf{VS})^2 \text{ , m=1…M} \tag{3}$$

with $\mathrm{g_m}$ being the $\mathrm{m^{th}}$ object signature and M the total number of vortex objects in the frame under processing. The extracted vortex ring is then defined as the vortex structure with the minimum $\boldsymbol{D_{sig}}$.

6.3. Experiments

6.3.1. Data and Preprocessing

The proposed method was evaluated on a data from eight healthy volunteers (mean age: 40±15 years) who underwent three-dimensional (3D), time resolved, three-directional Phase Contrast (VE) MR imaging at 1.5 T (Philips). VE MRI was performed in a 3D isotropic dataset of 4.2×4.2×4.2mm^3 covering all 4 cardiac chambers. Retrospective gating with 30 phases with average temporal resolution of 30 ms were reconstructed and velocity sensitivity of 150cm/s in all directions were used. This data was then linearly interpolated spatially to result in a 1 mm^3 spatial resolution. The whole heart (not just the LV) region was then outlined manually from all slices and time frames. There are two reasons behind segmenting the whole heart region instead of just the LV. First, to investigate the ability of our method in extracting the LV vortex rings in the presence of other vortex structures formed in other ventricles. Second, to avoid the need for LV segmentation from the PC-MRI magnitude images (Figure 6.1. b and d) which usually suffer from low contrast between LV and right ventricle (RV) boundaries making LV segmentation a difficult task.

6.3.2. Diastolic Vortex Ring Extraction

Using the manually segmented whole heart flow field volumes resulting from the previous step, vortex structures were identified using the Lamda2 method. After Applying threshold T_{λ_2} (as explained in Sec. 2.1), connected component analysis method (CCA) [14] was then applied to define the identified vortices as connected vortex objects. After that, LV vortex rings were labeled manually to be used as ground truth. In this work, for each subject, two observed rings were labeled from each of the rapid early (**E**) and late filling (**A**) diastolic phases. The two early filling rings correspond to the rings of the peak early filling PC-MRI phase and the subsequent frame. Similarly, the two late filling rings were labeled from the peak late filling phase and the subsequent frame. These were the frames in which vortex rings were observed consistently in all 8 subjects. From the eight volunteers, in total 32 LV vortex rings were manually labeled which then used as the ground truth to evaluate the proposed extraction method. For computing the Laplace-Beltrami (LB) signature [13], the vortex shape signature is captured from the Lambda2 isosurfaces with T_{λ_2} as isovalue.

To quantitatively evaluate the proposed method and to avoid bias in the selection of the average signature **VS**, a leave-one-out cross-validation approach was used. The average signature **VS** was computed from 7 subjects out of the available 8 subjects (i.e. computed as average of the corresponding 28 vortex signatures). This **VS** is then used to extract the LV vortex rings from the 4 aforementioned frames of the left out subject. This is repeated 8 times, leaving out different subjects. To evaluate the extraction performance we used the precision criterion, which was computed as the proportion TP/(TP+FP) where TP stands for the true positive i.e. the number of correctly extracted LV vortex rings, FP for false positive i.e. the number of the mis-extracted LV vortex rings.

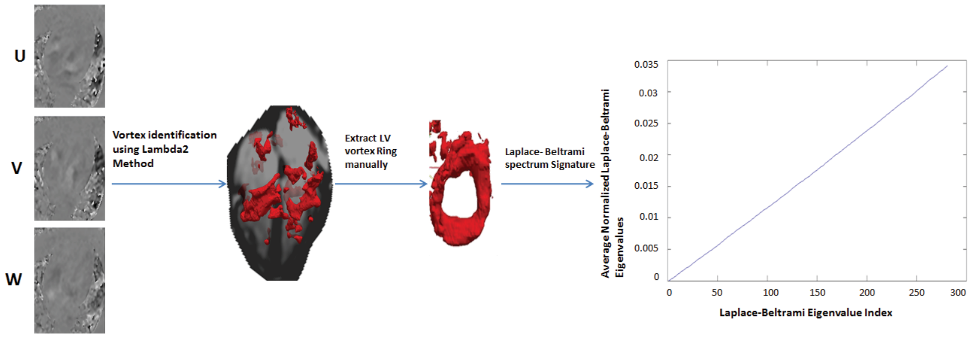

Figure 6.2. Steps of the proposed vortex ring shape signature extraction from one subject, U, V, W are three volumes representing the PC-MRI flow field velocity components.

6.3.3. Parameter selection

In the proposed method there are two empirically determined parameters, T_{λ_2} and $\boldsymbol{d}$. T_{λ_2} is application and subject specific. In this study, T_{λ_2} was manually adjusted per subject until meaningful vortex rings could be differentiated from surrounding structures. In our experiments**,** T_{λ_2} in the range of **[2-5]** μ (with μ as the λ_2 average of voxels with λ_2 <0) was found to give good results. Second, in the applied Laplace-Beltrami analysis, a signature of 300 eigenvalues (i.e. $\boldsymbol{d}$=300) was sufficient in all experiments.

6.4. Results

The overall precision is 0.844, detailed results for the performance over the two diastolic phases are given in Table 6. 1, where every phase has a total of 16 LV transmitral vortex rings to be extracted. In the reported results, vortex rings were extracted from an average of 43 different sized surrounding vortex structures in the **E**-phases and an average of 30 structures in the **A**-diastolic phases. The proposed method failed in extracting only 5 rings, 1 from the **E** phase and 4 from **A**, out of the total 32 vortex rings.

Table 6. 1. LV Transmitral vortex ring extraction results

Phase	E (n=16)	A (n=16)	Total (n=32)
True Positive	15	12	27
False Positive	1	4	5

6.5. Discussion and Conclusion

Our results show that the proposed cardiac-vortex-specific signature based extraction is rather accurate in extracting LV diastolic transmitral vortex rings from whole heart PC-MRI with 27 successfully extracted LV vortex rings out of the total 32 rings yielding an overall precision of 0.844. In all 5 failed cases, the proposed algorithm extracted the RV C-shape or incomplete rings instead of the LV ring i.e. it was successful in ring extraction but could not differentiate between the RV partial rings and the more complete LV vortex rings. This could be due to the similarity in shape (e.g. curvature and complexity) of RV and LV vortex rings. Moreover, in all failed experiments, the LV vortex ring was ranked second after the RV partial ring based on the distance defined in Eqn.3 with a small difference of 0.16 ± 0.23 from the highest rank while the third ranking structure (not ring) was more distant (2.72 ± 1.90) from the highest ranking structure. It is important to note that the proposed **E**-phase trained average signature was able to detect most of the **A**-phase rings (12 out of 16), which shows the ability of the proposed method to deal with shape variability of the transmitral vortex rings between the **E** and **A** diastolic phases. The proposed method is automatic relative to the LV vortex ring extraction process. In this work, the whole heart region was still segmented manually from PC-MRI as automatic segmentation is out of this paper's focus. On the other hand, vortex identification is a complex fluid dynamics topic and no definite rigorous vortex definition is yet reached. In this work, we used the Lambda2 method which is the most commonly accepted fluid dynamics definition of a vortex [1]. Nevertheless, this method requires definition of T_{λ_2} threshold for defining meaningful vortex structures. To the best of our knowledge, no objective method has been reached yet for defining T_{λ_2}. Currently, we are working on developing a method for objective definition of this threshold. For the LB signature normalization, we evaluated different normalizations as suggested in [13], however, the best normalization in our case was to normalize by both the signature's fitting line slope and the vortex volume.

To our knowledge, this is the first attempt to automatically extract transmitral vortex rings from PC-MRI in general and from the LV in particular. Our results show that the proposed method is a promising technique for left ventricular vortex ring extraction. Furthermore, the results show the capability of the proposed method dealing with the vortex ring shape differences between the two diastolic (**E** and **A**) phases**.** As such, this work can be seen as a first step towards a quantitative understanding of cardiac vortex structures, their evolution and physiological implications. In addition, the proposed method could be used for vortex ring analysis in CFD simulations.

6.6. References

1. Kheradvar, A. and G. Pedrizzetti, Vortex formation in the cardiovascular system. 2012, Springer. p. 45-53.
2. Charonko, J.J., et al., Vortices formed on the mitral valve tips aid normal left ventricular filling. Annals of biomedical engineering, 2013. 41(5): p. 1049-1061.
3. Le, T.B. and F. Sotiropoulos, On the three-dimensional vortical structure of early diastolic flow in a patient-specific left ventricle. European Journal of Mechanics-B/Fluids, 2012. 35: p. 20-24.
4. Domenichini, F., G. Pedrizzetti, and B. Baccani, Three-dimensional filling flow into a model left ventricle. Journal of fluid mechanics, 2005. 539: p. 179-198.
5. Jiamsripong, P., et al., Impact of Acute Moderate Elevation in Left Ventricular Afterload on Diastolic Transmitral Flow Efficiency: Analysis by Vortex Formation Time. Journal of the American Society of Echocardiography, 2009. 22(4): p. 427-431.
6. Kheradvar, A., et al., Assessment of transmitral vortex formation in patients with diastolic dysfunction. Journal of the American Society of Echocardiography, 2012. 25(2): p. 220-227.
7. Töger, J., et al., Vortex ring formation in the left ventricle of the heart: analysis by 4D flow MRI and Lagrangian coherent structures. Annals of biomedical engineering, 2012. 40(12): p. 2652-2662.
8. Eriksson, J., et al., Semi-automatic quantification of 4D left ventricular blood flow. J Cardiovasc Magn Reson, 2010. 12(9): p. 12.
9. Markl, M., et al., Time-resolved three-dimensional magnetic resonance velocity mapping of aortic flow in healthy volunteers and patients after valve-sparing aortic root replacement. The Journal of thoracic and cardiovascular surgery, 2005. 130(2): p. 456-463.
10. Morbiducci, U., et al., In vivo quantification of helical blood flow in human aorta by time-resolved three-dimensional cine phase contrast magnetic resonance imaging. Annals of biomedical engineering, 2009. 37(3): p. 516-531.
11. ElBaz, M.S., et al., Quantification of diastolic vortex shape deformation in left ventricular filling from 4D flow MRI. Journal of Cardiovascular Magnetic Resonance, 2013. 15(Suppl 1): p. P79.
12. Jeong, J. and F. Hussain, On the identification of a vortex. Journal of fluid mechanics, 1995. 285: p. 69-94.
13. Reuter, M., F.-E. Wolter, and N. Peinecke, Laplace–Beltrami spectra as 'Shape-DNA'of surfaces and solids. Computer-Aided Design, 2006. 38(4): p. 342-366.
14. Haralock, R.M. and L.G. Shapiro, Computer and robot vision. 1991: Addison-Wesley Longman Publishing Co., Inc.